ELSEVIER

Catena 50 (2003) 469–487

CATENA

www.elsevier.com/locate/catena

Energy formulations of head cut dynamics

S.N. Prasad[a,*], M.J.M. Römkens[b]

[a] Department of Civil Engineering, University of Mississippi, University, MS 38677, USA
[b] USDA ARS National Sedimentation Laboratory, Oxford, MS 38655, USA

Received 29 September 2000; received in revised form 4 February 2002; accepted 23 July 2002

Abstract

This study employs the principles of energy conservation to establish the framework for the development of the dynamical equations of head cut as a part of a continuum mechanical analysis of soil erosion induced by surface flow. The dynamics of head cut are controlled by several physically distinct processes, notable among which are surface seal formation, its failure and the redistribution of flow energy into kinetic and dissipation energies of water and soil. Thus, an erosive energy release rate function is introduced in the global energy equation, which is shown to depend on physical parameters governing the dynamics of the process region. The energy release rates are decomposed into line integrals representing motions associated with the translation, rotation, self-similar expansion and the distortion of the head cut cavity. From these considerations, approximate analytical expressions are derived which establish criteria for the initiation and the steady state head cut velocity. The results at this stage of development are preliminary and need testing and validation with data under controlled experimental conditions.

Keywords: Head cut; Surface seal; Soil erosion; Shallow flow; Erosion energy

1. Introduction

Considerable mathematical difficulties exist in the determination of erosion and sediment transport rates due to concentrated flows near head cuts and gullies. Although an overall functional boundary value problem may be formulated to describe the process region of head cut, an exact solution of such a nonlinear integro-differential equation will be an unrealistic expectation. Moreover, the shape and size of the boundary within which erosion and sediment transport processes take place are not beforehand known, thus, making the problem further mathematically intractable. In the past, several studies have been conducted to understand the fluid dynamics of free fall under a step change in the surface slope, which elucidated the flow structure hydraulic parameters (Moore, 1943;

* Corresponding author.

PII: S0341-8162(02)00125-X

Henderson, 1965). These studies have helped in understanding the development of tractive forces on the rigid boundary as well as the accompanying effects when boundary conditions near the fall are changed. They are also useful in understanding the roles of various parameters in the initiation of the erosion process and its short term or transient characterization. A sustained growth of head cuts and the resulting sediment transport rates, however, are believed to be primarily energetic in nature where the energy redistribution between the flow and the soil mass becomes the controlling mechanism. Energy is released from the surface flow, which is then used in the erosion and entrainment processes and further converted into kinetic energy of the flow and in the transport of eroded materials. A part of the energy is also utilized in the propagation of the newly created boundary of the head cut.

This paper, therefore, explores in a systematic way the various conservation laws which may be utilized to circumvent the complexities present in the interacting subprocesses of head cut dynamics. The inspiration for this approach lies in the success which researchers have found in the areas of nonlinear wave propagation in fluids (Witham, 1973). The exchange of energy in the process region is formulated into suitable forms which are shown to lead to certain closed form solutions. One solution establishes the bounds of the velocity for steady state head cut motion, whereas the other solution yields a criterion for its initiation.

2. Energy model formulation

Energy principles have long been used as a means to investigate problems of continuum mechanics of deformable bodies. Along with the subject of variational calculus, these principles have greatly helped the understanding of complicated dynamic systems especially when subprocesses in the systems, such as those involving nonlinearity of material properties, local singularities and strong fluctuations, etc., become complex due to strong interactions between sources and sinks in the system. In order to bypass a detailed analysis of this complicated problem, the concept of energy release rate in the process region is introduced. In the general case, this consists of a surface integral which for two-dimensional analysis (as in a flume study) reduces to a line integral. The choice of the line integral is somewhat arbitrary but is chosen such that it surrounds the head cut cavity thereby directly integrating the locally varying parameters. The line integrals are amenable to numerical evaluation and yield informations on head cut growth rates as will be seen below.

The subject of soil erosion by overland flow may, in its simplest manifestation, be viewed as an interaction problem between the hydrodynamics of the flow and the underlying surface soil matrix with its constitutive properties. The process region is primarily limited to the zone near the soil surface. In some locations, this process seems to take place in a uniform manner (Fig. 1A); at others it is concentrated, leading to discontinuities (head cuts) which move upstream as a result of that part of the energy that is expended by concentrated flow on the surface soil matrix (Fig. 1B). Thus, the energy source of the system is derived from the flow, whereas the energy sink lies in the process of soil detachment, entrainment and removal of the soil and water from the surface in general, or specifically from the head cut region. In order to formulate the problem of the eroding head cut, the case of a soil of which the original surface is denoted by $X_2 = 0$ (Fig. 1A and B) is considered. This surface supports a concentrated flow regime with time

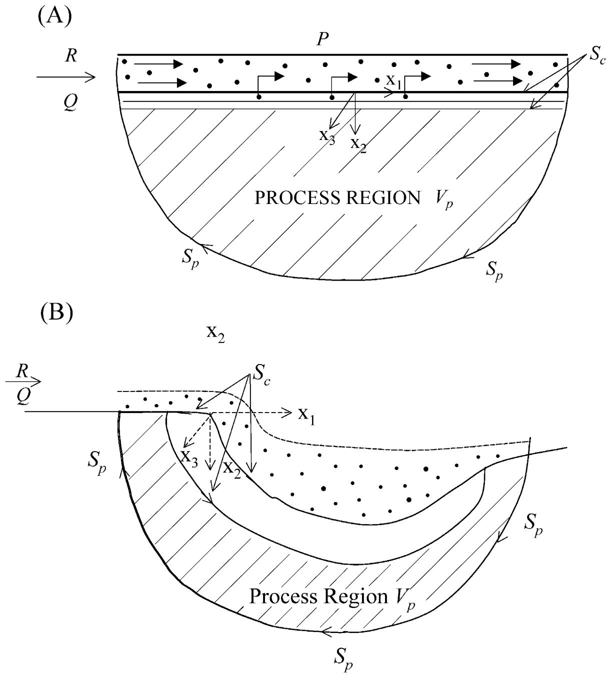

Fig. 1. A schematic representation of the process region of an eroding surface: (A) for an uniform surface and (B) for a head cut region.

rate of flow energy per unit volume given by R (Fig. 1). Let P be the time rate of energy responsible for the detachment of soil, and let Q be the heat energy per unit time of flow that enters the process region. Assume further that T and E are, respectively, the total kinetic and internal energies of the detached soil mass originally bounded by an arbitrary surface S_p denoted in part by $X_2 = 0$ (Fig. 1). (E is a temperature-dependent quantity, a factor rarely considered in soil erosion research). The energy partitioning mechanism in the process region assumes that the flow energy is transmitted to the soil surface by means of an equivalent tractive force vector $\boldsymbol{F}_i$, ($i = 1,2,3$). The generality of this approach is self-evident by considering the general three-dimensional problem in which the domain of the soil mass is given by $X_2 \geq 0$. In this paper, the indicial notation with a repeated index denotes a summation and a dot over a variable implies the time rate of change.

As suggested in this model (Fig. 1), the process region is assumed to be homogeneous and uniformly eroding and bounded by the surfaces S_p and S_c. Thus, P may be viewed as the rate at which energy is required to detach soil in the process region represented by V_p. The system's energy balance equation in the region V_p bounded by S_p may then be given by:

$$R + Q = \frac{dT}{dt} + \frac{dE}{dt} + P + H' \tag{1}$$

where H' represents energy rate associated with seepage, rainfall, etc. While the latter contributions may be very significant, they are not considered in this exercise on head cut analysis. The time rates of flow and heat energies may be represented by:

$$R = \int_{S_p} \boldsymbol{T}_i \dot{\boldsymbol{u}}_i \mathrm{d}S + \int_{V_p} \boldsymbol{f}_i \dot{\boldsymbol{u}}_i \mathrm{d}V \tag{2}$$

$$Q = \int_{S_p} (-\boldsymbol{q}_i \boldsymbol{n}_i) \mathrm{d}S + \int_{V_p} \rho\gamma \mathrm{d}V \tag{3}$$

where $\boldsymbol{u}_i$ and $\boldsymbol{f}_i$ are the displacement and body force vectors, respectively; $\boldsymbol{q}_i$ is the heat flux vector; γ is the heat produced by internal heat sources; ρ is the mass density and $\boldsymbol{n}_i$ is the outward unit normal vector to the surface S. The integral signs with S_p and V_p are surface and volumetric integrals, respectively.

The time rate of change of the total kinetic energy equals the total time rate of change of the kinetic energy density in V_p plus the flux of kinetic energy density out of the boundary surface of V_p, i.e.

$$\frac{\mathrm{d}T}{\mathrm{d}t} = \int_{V_p} \rho \dot{K} \mathrm{d}V + \int_{S_p} \rho K \boldsymbol{V}_i (-\boldsymbol{n}_i) \mathrm{d}S \tag{4}$$

where K is the kinetic energy per unit mass, $\boldsymbol{V}_i$ is the velocity vector and $\boldsymbol{n}_i$ is the outward unit normal vector of the surface S_p. Similarly, the time rate of change of the internal energy is given by the relationship:

$$\frac{\mathrm{d}E}{\mathrm{d}t} = \int_{V_p} \rho \dot{e} \mathrm{d}V + \int_{S_p} \rho e V_i (-\boldsymbol{n}_i) \mathrm{d}S \tag{5}$$

where e is the internal energy per unit mass. Outside the process region, the deformations are assumed to be infinitesimal so that there, the linear equations of continuum mechanics are valid. These equations are (Eringen, 1980):

$$t_{ij,j} + f_i = \rho \ddot{\boldsymbol{u}}_i \tag{6}$$

$$e_{ij} = 1/2(u_{i,j} + u_{j,i}), \quad V_i = \dot{\boldsymbol{u}}_i \tag{7}$$

$$\rho \dot{e} = t_{ij} \dot{e}_{ij} + \boldsymbol{q}_{i,i} + \rho\gamma \tag{8}$$

$$\rho \dot{K} = \rho \ddot{\boldsymbol{u}}_i \dot{\boldsymbol{u}}_i \tag{9}$$

$$\boldsymbol{T}_i = t_{ij} \boldsymbol{n}_j \tag{10}$$

where t_{ij} is the stress tensor and e_{ij} is the infinitesimal strain tensor. The set of Eq. (6) represents the balance of linear momentum, whereas Eq. (8) is derived from the conservation of energy principles in which e represents the internal energy density. The components of surface traction $\boldsymbol{T}_i$ are obtained in terms of the stress tensor t_{ij} from Eq. (10), where $\boldsymbol{n}_i$ is the outward unit normal. The above separation of the energies in the form of fluxes moving with velocity V_i makes it possible to derive the detachment energy rate P. This is accomplished by substituting Eqs. (3)–(5) into Eq. (1), followed by the application of the Gauss Theorem to change the volume integral term into a surface integral term. The resulting equations simplify considerably by utilizing the linear equations of continuum mechanics given by Eqs. (6)–(10), which yields:

$$P = \int_{S_c} \{\rho(K + e)V_i \boldsymbol{n}_i + \boldsymbol{T}_i \dot{\boldsymbol{u}}_i - \boldsymbol{q}_i \boldsymbol{n}_i\} \mathrm{d}S \tag{11}$$

The erosive energy or detachment rate given by Eq. (11) is a general expression and should therefore be a widely applicable relationship. It should be mentioned that although Eq. (11) is derived by satisfying the set of field equations (Eqs. (6)–(10)) which are linear, no linearity assumption is essential in the process region and, therefore, the integral theorem given by Eq. (11) will admit any physically admissible constitutive law. The first two terms on the right hand side of Eq. (11) represent fluxes of kinetic and internal energies in the process region, whereas the third term is the thermal energy fluxes. The growth and the deformation of the head cut cavity directly affect the magnitude of these fluxes, and therefore, in the following section, we investigate the dynamical kinematics of head cut developments.

3. Components of energy release in head cut processes

The generalized energy balance equation applies to all forms of soil erosion by water. However, real world situations involve soil heterogeneity, nonuniform and unsteady flows, which lead to uneven changes in the geometry of the eroding soil surface, often manifested as head cuts. In those situations, the application of the energy balance equation becomes extremely complicated and is best approached by allocating proportionately the flow-released energy to the components of geomorphic changes of the growing and migrating head cuts. These components of the moving head cuts consist of translational, rotational, self-similar expansion and distortional (non-self-similar) motions (Fig. 2). In order to make these energy allocations, we present a general analysis, using a moving coordinate system, that simulates in a schematic manner how geomorphological differences in erosional responses, including head cuts, may be understood. In this analysis, the origin coincides with the tip (0) of the head cut (Fig. 3). These coordinate systems are a moving translational frame $(0 - x_1,x_2)$ and a rotational frame $(0 - r,\theta)_3$ both moving with the head cut velocity, V_c. The rotational frame has an angular velocity ω_3. The kinematic details of transcribing these motions into these coordinate systems can be quite complicated, even for a system with two coordinates, which is applicable in most experimental head cut studies in the laboratory. The following analysis assumes a planar model in the

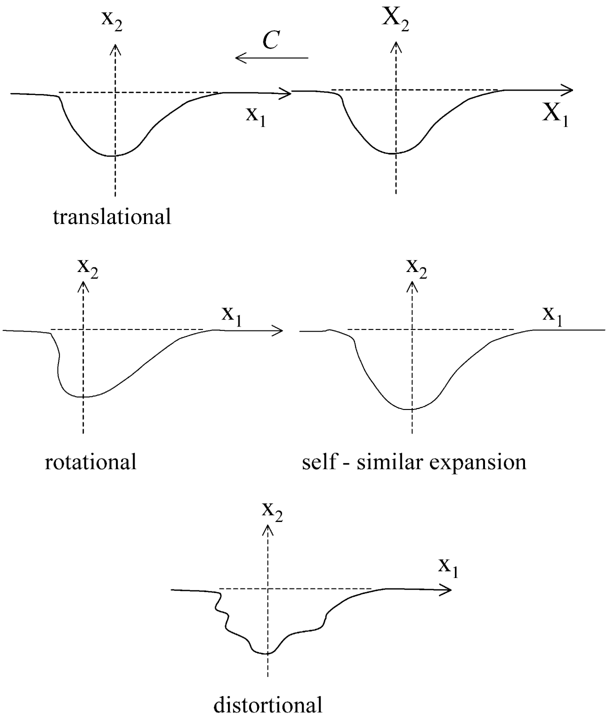

Fig. 2. A schematic representation of the geomorphic components of a moving head cut.

X_1–X_2 plane (Fig. 4). The position of a point B on the head cut surface S_c at time $t=t_0$ is denoted by a vector $\vec{r}(\theta, t_0)$, that extends from the tip 0 to the point B. After an incremental time increase Δt, the head cut has propagated over a distance and the deformation of the domain S_c, the head cut region, has moved along a rather arbitrary but smooth trajectory as indicated in Fig. 4. We select a point, say b, on the new curve S_c in such a way that the numerical value of the moving angular coordinate θ of the point is the same as that of the

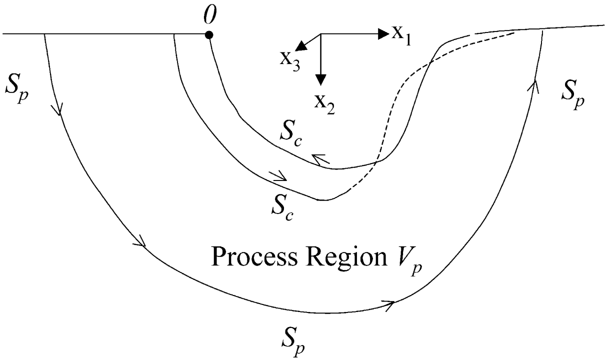

Fig. 3. Cross-section of the head cut process region V_p.

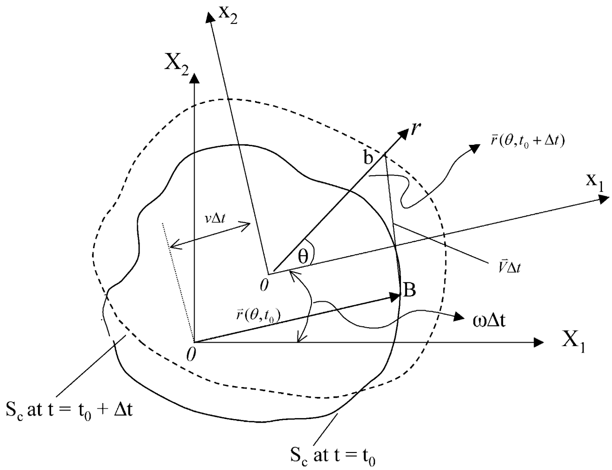

Fig. 4. A schematic representation of the displacement of a point *B* on the head cut surface as described by a moving coordinate system.

point *B*. The point *b* is represented by a vector $\vec{r}(\theta, t_0 + \Delta t)$ as shown in Fig. 4. We define the velocity of S_c, as $\vec{V}(\theta, t_0)$ as

$$\vec{V}(\theta, t_0)\Delta t = \vec{v}\Delta t + \vec{r}(\theta, t_0 + \Delta t) - \vec{r}(\theta, t_0) \tag{12}$$

As shown in Fig. 4, $\vec{V}\Delta t$ is the vector connecting the points *B* and *b*. Letting $\Delta t \to 0$ we obtain

$$\vec{V} = \vec{v} + \frac{\partial \vec{r}}{\partial t} = \vec{v} + \frac{\partial}{\partial t}(r\vec{e}_r)$$

i.e.

$$\vec{V} = \vec{v} + r\frac{\partial}{\partial t}\vec{e}_r + \frac{\partial r}{\partial t}\vec{e}_r \tag{13}$$

where r is the length of $\vec{r}$ and $\vec{e}_r$ is a unit vector having the same direction as $\vec{r}$.

In order to separate energies associated with translation, rotation, expansion and deformation, we consider in Fig. 5, schematically, the shapes of S_c at time $t = t_0$ and $t = t_0 + \Delta t$, which are viewed from the moving frame $(0 - x_1, x_2)$. Since the values of the moving angular coordinate θ of the point *b* is the same as that of *B*, the points 0, *B* and *b* are observed as if they were on a straight line. The points B^* and b^* in Fig. 5 correspond, respectively, to the points *B* and *b* in Fig. 4. The shape of the thinly drawn curve in Fig. 5 is similar to that of the solid curve, i.e. S_c at $t = t_0$, while the area within the thin curve is the same as that of the dashed curve, i.e. S_c at $t = t_0 + \Delta t$. The point H^* is the intersection of the thin curve and the line $\overline{0b^*}$. Since

$$0b^* - 0B^* = B^*H^* + H^*b^*$$

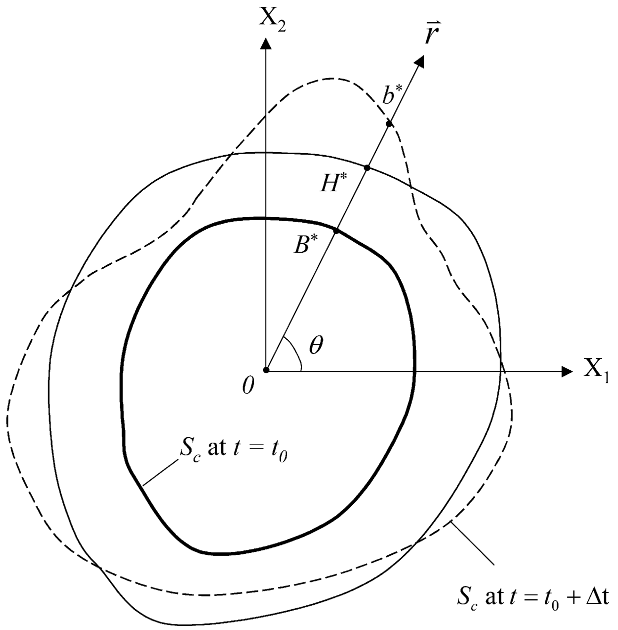

Fig. 5. A schematic representation of a growing and deforming head cut during a time interval Δt.

we may obtain

$$r(\theta, t_0 + \Delta t) - r(\theta, t_0) = ar(\theta, t_0)\Delta t + h(\theta, t_0)\Delta t \tag{14}$$

where $h(\theta,t_0)$ is a constant representing the extent of non-self-similar distortion and $ar(\theta,t_0)\Delta t$ is the length B^*H^*. The constant a, on the other hand, is a deformation constant representing the extent of self-similar distortion and is determined by equating the area within the thin curve to that within the dashed curve, i.e.

$$\int_0^{2\pi} r^2(\theta, t_0 + \Delta t)\mathrm{d}\theta = (1 + a\Delta t)^2 \int_0^{2\pi} r^2(\theta, t_0)\mathrm{d}\theta \tag{15}$$

The length H^*b^* is denoted by $h(\theta,t_0)\Delta t$. In the limit $\Delta t \rightarrow 0$, we obtain from Eqs. (14) and (15)

$$\frac{\partial r}{\partial t} = ar + h \tag{16}$$

where

$$a = \frac{\displaystyle\int_0^{2\pi} \frac{\partial r^2}{\partial t} \mathrm{d}\theta}{\displaystyle 2\int_0^{2\pi} r^2 \mathrm{d}\theta} \tag{17}$$

For conditions in which soil cohesion is small, energy associated with deformations (non-self similar) will be small in comparison with the other dissipation energies. Thus, in the following case, we will assume $h = 0$. The boundary velocity $\vec{V}$, relationship (13), now yields

$$\vec{V} = \vec{v} + \omega_3 x\vec{r} + a\vec{r} \tag{18}$$

It is seen from Eq. (18) that $\boldsymbol{V}_i$ decomposes into the components of translation with velocity v_i, the rotation with angular velocity ω_3, and the self-similar expansion, expressed by the parameter a, of the process region of the head cut. Combining Eq. (18) with Eq. (11), we obtain

$$P = v_i J_i + \omega_3 L_3 + aM \tag{19}$$

where

$$J_i = \int_{S_c} \left\{ \rho(\kappa + e)\boldsymbol{n}_i - T_j \frac{\partial \boldsymbol{u}_j}{\partial x_i} \right\} \mathrm{d}s \tag{20}$$

$$L_3 = \int_{S_c} e_{i3e} x_c \left\{ \rho(\kappa + e)\boldsymbol{n}_i - T_j \frac{\partial \boldsymbol{u}_j}{\partial x_i} \right\} \mathrm{d}s \tag{21}$$

$$M = \int_{S_c} X_i \left\{ \rho(\kappa + e)\boldsymbol{n}_i - T_j \frac{\partial \boldsymbol{u}_j}{\partial x_i} \right\} \mathrm{d}s \tag{22}$$

It is noted that J_1, L_3 and M are the components of the energy release rates associated with the translation, rotation and self-similar expansion, respectively. These integrals, however, are line integrals which enclose the process region but have similarities with those which appear in studies of crack propagation in solids. In solid mechanics, those integrals lead to path-independent integrals (Budiansky and Rice, 1972; Freund, 1972) which form a powerful basis for solutions of nonlinear crack propagation problems. Similarly, integrals given by Eqs. (20)–(23) may be converted by Gauss' theorem to forms over the regular region outside the process region such that their numerical evaluations for phenomenologically nonlinear effects could be accomplished.

4. Head cut models

In general, head cuts may grow in a variety of ways involving quite complicated mechanisms whose origins may be in certain inherent, dynamic instabilities. The first model assumes surface flow in which individual particles are detached from the surface of the soil which idealistically is considered to be homogeneous. This is the most commonly assumed case illustrated in Fig. 6a. In this model, erosion rates may be estimated based on excess tractive force or stream power over a certain critical value. These critical values

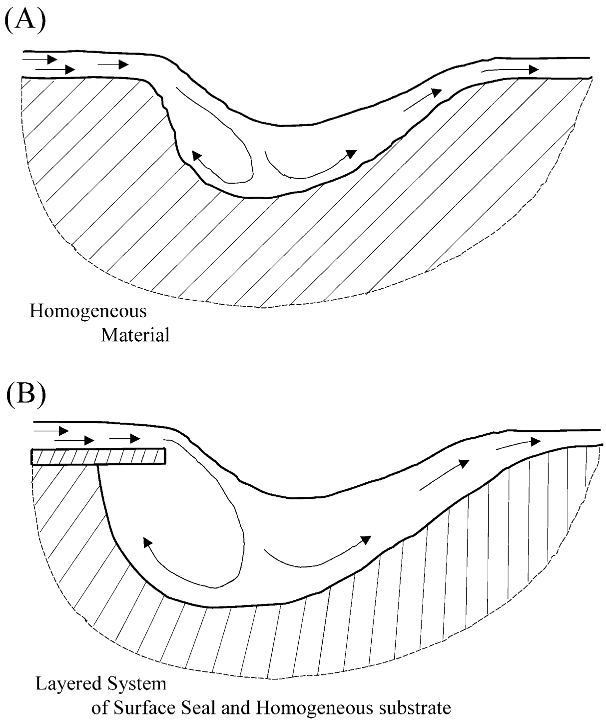

Fig. 6. Graphical representation of two modes of head cut erosion: (A) case of homogeneous material and (B) case of heterogeneous material of a developed surface seal over a homogeneous substrate.

have been the subject of extensive research but no definite procedure has been devised yet for its determination and, therefore, has remained an empirical consideration. The second model, shown in Fig. 6b, is a layered system consisting of a compact, cohesive surface layer on top of a significantly less-cohesive, or often a nearly cohesionless, substrate. Only the latter case is considered in this paper. It represents situations that are often observed on agricultural fields where tilled soil develops a seal during rainfall, which subsequently breaks down by surface or concentrated flow, thereby forming head cuts or approximate stepwise changes in the surface topography. In this model, two contributing factors are considered and have been observed in laboratory studies (Bennett et al., 2000). One factor may lead to a chipping (surface) mode failure caused by crack propagation in the surface seal. The second factor is due to propagation of debonding between the surface seal and the substrate material due to the soil removal by the flow. Head cut growth involves both modes with comparable participation. The hydrodynamics of surface flow primarily controls the extent of these operational mechanisms but soil properties and the geomorphology of the head cut specifics are also contributing factors. The study of layered system failure involves assessing the stress distribution in the seal layer caused by the various forces acting on the seal and due to the weakening of the substrate when the pore pressure between the seal and the substrate becomes less negative or positive. Since the theme of this paper concerns the mechanical analysis of this process, certain intrinsic instability mechanisms will be first discussed.

The study will first focus on the stability behavior of head cut growth. The conceptual model is based on an analysis of balance of energy represented by a special case of Eq. (11). The special case is obtained in the limit of equilibrium when dynamic forces are zero. In this situation, we will assume that the thickness of the seal is h and the bonding force between the seal and the substrate is negligible, but seal and substrate are held together by interfacial capillary tension. The substrate material is cohesionless and is readily entrained and transported by the surface water when the interstitial suction is lost. We will further assume that the separation length over which the seal is simply resting without any resistance from the substrate against vertical deflection of the seal is ℓ (Fig. 7). The situation may, therefore, be modeled as a beam of width unity with an overhang of length ℓ and thickness h (Fig. 7). Furthermore, the seal is subjected to self-weight and the weight of flowing water and it will be assumed that the hydrodynamic force of the flowing water is equivalent to a thrust of magnitude F due to the jet effect acting at an angle φ with the

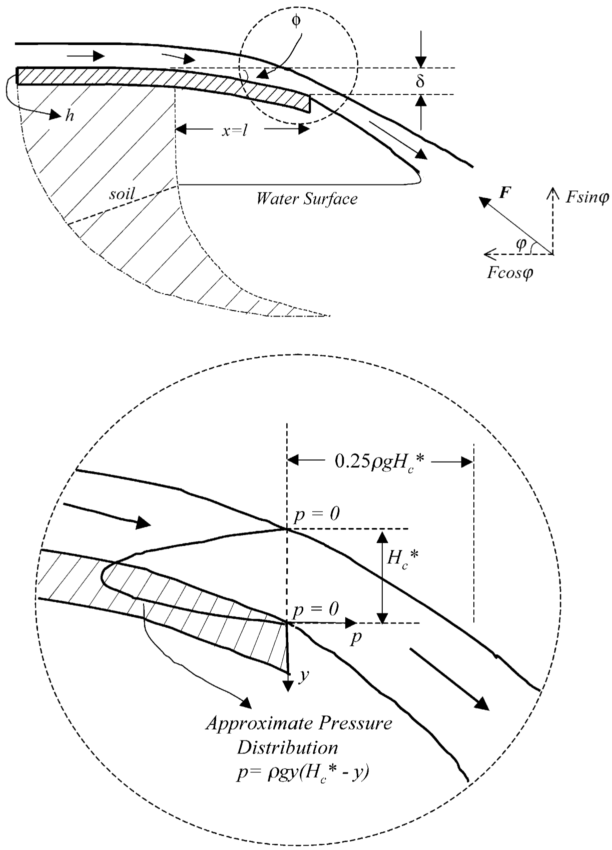

Fig. 7. A schematic representation of the flow field and a bending seal in the head cut region.

horizontal direction. In order to apply the principle of balance of energy to this problem, the various energy sources (gravity) and sinks (plastic hinge) and a failure mechanism must be identified. A plausible mechanism of seal failure is that the energy storing bending stress which is maximum near the support $x=\ell$ gives rise to a plastic hinge. A plastic hinge in a rectangular ($b \times h$) beam is formed when the top or bottom half of the cross-section is fully stressed up to yield stress σ_y in either tension or compression. The plastic moment (ultimate) is then given by $1/4bh^2\sigma_y$. At the maximum bending stress, the value of which depends on the seal mechanical properties and the hydrodynamic forces of the flow, an ultimate (plastic) bending moment develops. In this limiting state, the energy balance Eq. (11) when simplified yields:

$$W - V = 0 \tag{23}$$

where W is the work done by all external forces and V is the sum of all energies either stored (strain energy) or dissipated in yielding (i.e. at a hinge). W primarily consists of the work W_1 done by the superimposed total weight and the work W_2 of the thrust F. The quantifying relationships for W_1 and W_2 are, respectively:

$$W_1 = \int_0^{\ell} qy \, \mathrm{d}x \tag{24}$$

$$W_2 = \int_0^{\ell} F\cos\varphi \mathrm{d}x - F\delta\sin\varphi \tag{25}$$

where

$$q = q_0 + \rho g H \tag{26}$$

in which q_0 is the weight per unit length of the seal, ρ is the mass density of water, H is the average water depth of flow, g is the acceleration due to gravity, y and x are coordinates with the origin located at the "hinge" point, and δ is defined in Fig. 7. The vertical deflection of the section x is given by y such that at the tip ($x=0$), the deflection equals $\delta=y(0)$. Thus,

$$W = \int_0^{\ell} (q_0 + \rho g H) y \mathrm{d}x + \int_0^{\ell} F\cos\varphi \mathrm{d}x - F\delta\sin\varphi \tag{27}$$

The strain energy U_1 stored in the seal is given by

$$U_1 = \frac{1}{2E_y I} \int_0^{\ell} M^2 \mathrm{d}x \tag{28}$$

where M is the bending moment at the section x and $E_y I$ is the flexural rigidity of the seal. E_y is the Young's modulus of elasticity and I is the moment of inertia. Similarly, the strain energy U_2 in the substrate due to compression by the weight of the overlying seal may be calculated. The energy U_3 in the plastic hinge for a rotation under angle Φ at $x=\ell$ is given by

$$U_3 = M_u \Phi \tag{29}$$

where Φ is defined in Fig. 7, and M_u is the ultimate moment (plastic moment) of the seal of unit width and is given by

$$M_u = \frac{1}{4}\sigma_y h^2 \tag{30}$$

where σ_y is the yield stress of the seal material. Thus, the sum of all energies either stored (strain energy) or dissipated in a failure mechanism is given by:

$$V = U_1 + U_2 + U_3 \tag{31}$$

so that the energy balance equation given by Eq. (23) yields:

$$\int_0^\ell (q_0 + \rho g H) y \mathrm{d}x + \int_0^\ell F\cos\varphi \mathrm{d}x - F\delta\sin\varphi = \frac{1}{2E_y}\int_0^\ell M^2 \mathrm{d}x + U_2 + M_u\Phi \tag{32}$$

Eq. (32) may be viewed as the stability equation from which the nature of the dynamic states may be determined (Timoshenko and Gere, 1961) by investigating the bifurcation points in the phase plane (F–ℓ). Some insight into the roles played by the main parameters in determining the head cut dynamics may be gained by simplifying Eq. (32) to exclude secondary energy terms such as the strain energy U_1 and the compression energy U_2 of the substance. Furthermore, the integral relationship Eq. (24) may be simplified by integrating the work of gravity over the length of the overhang. This quantity is approximately given by the expression:

$$\int_0^\ell qy \, \mathrm{d}x \approx \frac{1}{2} q\ell\delta \tag{33}$$

so that Eq. (32) simplifies to yield:

$$\frac{1}{2} q\ell\delta + F\ell\cos\varphi - F\delta\sin\varphi = M_u\Phi \tag{34}$$

Upon solving Eq. (34) for F, one obtains:

$$F = \frac{1}{\cos\varphi - \frac{\delta}{\ell}\sin\varphi}\left(M_u\frac{\Phi}{\ell} - \frac{1}{2}q\delta\right) \tag{35}$$

If we further assume that $\delta \cong \Phi\ell$ (Fig. 7), where the tip deflection δ (Timoshenko and Gere, 1961) is given by:

$$\delta = \frac{q\ell^4}{8E_y I} = \Phi\ell \tag{36}$$

then Eq. (35) reduces to:

$$F = \frac{1}{\cos\varphi - \Phi\sin\varphi}\left(M_u\frac{q\ell^2}{8E_y I} - \frac{1}{2}q\frac{q\ell^4}{8E_y I}\right) \tag{37}$$

The critical thrust F_{cr} may be determined from Eq. (37) by letting $\partial F/\partial \ell = 0$ in Eq. (37). This yields:

$$\ell_{cr} = \sqrt{\frac{M_u}{q}} \tag{38}$$

from which the maximum thrust F_{cr} is given by:

$$F_{cr} = \frac{1}{16\cos\varphi} \frac{M_u^2}{E_y I} \tag{39}$$

When we substitute $M_u = 1/4(\sigma_y h^2)$ and $E_y I = E_y h^3/12$, Eq. (39) yields the critical horizontal thrust $H_{cr} = F_{cr}\cos\varphi$ as:

$$H_{cr} = \frac{3}{64}\left(\frac{\sigma_y}{E_y}\right)\sigma_y h \tag{40}$$

In effect, Eq. (40) determines the threshold condition for the head cut movement. Whenever the thrust F is larger than F_{cr}, the head cut will progress and for sufficiently large F, a steady condition may eventually take place. The problem is now reduced to determining F or H for a given flow field. Let us assume that the flow velocity on the overhang is in a critical flow condition. From hydraulic considerations (Henderson, 1965), the critical velocity V_c is approximately given as a function of the critical depth H_c according to the relationship:

$$V_c = \sqrt{gH_c} \tag{41}$$

We assume that the pressure distribution at the brink point $x = 0$ is parabolic with depth H_c^*. From hydraulic considerations (Henderson, 1965), the following applies:

$$\frac{2}{3} \preceq \frac{H_c^*}{H_c} \preceq 1 \tag{42}$$

The pressure distribution profile is as shown in Fig. 7 (inset). The magnitude of the thrust F, therefore, is given by the resultant of the parabolic pressure distribution and equals:

$$F = \frac{2}{3}\left(\frac{H_c^*}{4}\right)(H_c^*)\rho g \tag{43}$$

where ρ is the density of the fluid and g is the acceleration constant. If we assume further that $H_c^*/H_c = 2/3$ then the thrust F is given by

$$F = \frac{2}{27}\rho g H_c^2 \tag{44}$$

We will also assume that this thrust makes an angle φ with the horizontal direction. When Eq. (44) is utilized in Eq. (39), we obtain after some simplifications

$$V_c^2 = \frac{81}{128}\left(\frac{\sigma_y}{E_y}\right)\left(\frac{\sigma_y}{\rho}\right)\left(\frac{h}{H_c}\right)\frac{1}{\cos\varphi} \tag{45}$$

Eq. (45) is a very revealing relationship. It expresses the point of failure in terms of soil mechanical properties of yield stress and the modulus of elasticity and the physical flow properties of density and thickness of the surface layer on one hand and the critical flow field on the other. Eq. (45) is rather remarkable in the sense that once the mechanical property of the surface is evaluated, the critical flow field for seal breakup to occur may be determined by this relationship. It may also be noted that the three ratios on the right side of Eq. (45) have appeared in a way that is rather expected. The first two terms (σ_y/E) and (σ_y/ρ) are germaine to the mechanical response of the seal material, whereas the last term is flow case specific. Fig. 8 shows a schematic representation of this relationship for different flow regimes. It is hypothesized that this relationship should also be applicable for determining the condition of rill initiation in an overland flow situation when surface seals fail and rilling initiates.

The above analysis yields relationships of critical flow parameters and soil mechanical properties from which seal failure can be deduced. Once failure occurs, a new cycle of soil detachment and entrainment takes place, which is controlled by the hydrologic flow, the substrate water regime and intrinsic soil mechanical properties as embedded in the general expression of Eq. (11). Similar cycles of seal failure, soil detachment and entrainment were observed in rainfall-runoff studies with soil beds (see Römkens et al., 1997) These experimental studies revealed a high degree of surface seal failure instability which was

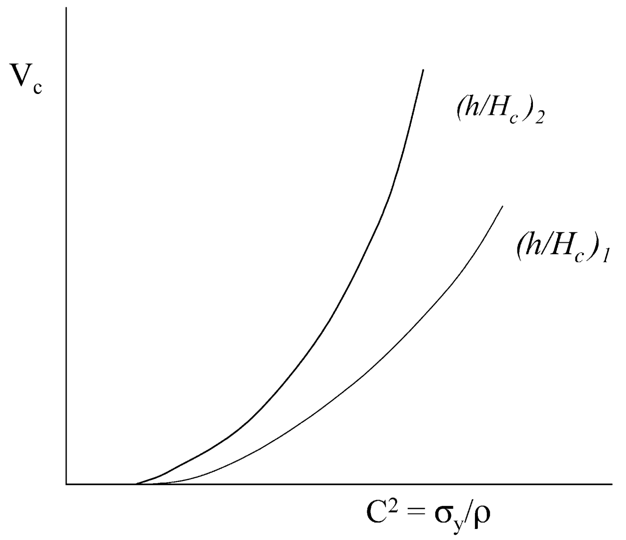

Fig. 8. A schematic representation of the relationship between the critical flow velocity and the surface seal property σ_y/ρ for different flow regimes.

followed by a rather catastrophic erosion event. It appears that there exist various bifurcation paths in the stability phase plane which may be further analyzed near the origin by the results based on Eq. (45).

5. An energy relationship application for head cut growth in cohesionless soil

We now consider the dynamic case of steady growth of head cut by an application of the general Eq. (11). We will neglect the thermal change and assume the head cut migration rate $\vec{V}$ is such that $V_2 = V_3 = 0$ and $V_1 = C$ is a constant. We further assume that there is no significant rotation of the cavity and, thus, only translational effect represented by C and deformational effect represented by S (introduced later) are retained in the analysis which follows. In the various experimental studies carried out in the past, head cuts are constrained more along the axis of the experimental setup, and therefore, results based on the above assumptions will be relevant in these cases. The angle φ was assumed to be the direction of thrust with the horizontal (Fig. 7). This angle $\varphi = \varphi_0 + \varphi_1$ where φ_1 is the angle of the centerline of the core of flow with the horizontal and φ_0 is the angle of the tangent to the brink with the vertical. These angles are dependent on the geometry of the head cut and the hydrodynamic conditions (Froude number) of the flow. The rate of work, W_2, supplied by the jet, therefore, is given by

$$W_2 = FC\cos(\varphi_0 + \varphi_1) \tag{46}$$

Let the cross-sectional area of the head cut be A so that the kinetic energy K_1 associated with the migration velocity of the head cut volume enclosed per unit width is given by:

$$K_1 = \frac{1}{2}\rho^* AC^2 \tag{47}$$

In the above, ρ^* is total mass density (soil + water) which includes the sediment mass also. For steady conditions, C may be assumed constant so that the time rate of the kinetic energy is:

$$\frac{\mathrm{d}}{\mathrm{d}t}\left(\frac{1}{2}\rho^* AC^2\right) = \frac{1}{2}\rho^* C^2 \frac{\mathrm{d}A}{\mathrm{d}t} \tag{48}$$

An estimate of $\mathrm{d}A/\mathrm{d}t$ may be made by assuming that entrainment of the soil into the flow takes place over a length S so that

$$\frac{\mathrm{d}A}{\mathrm{d}t} = SC \tag{49}$$

The conservation of energy principle states:

$$\frac{\mathrm{d}}{\mathrm{d}t}(\text{kinetic energy} + \text{internal energy}) = \text{Rate of work supplied} - \text{Rate of energy dissipation} \tag{50}$$

If one further simplifies the model by assuming that there is no significant loss in the internal energy, such as for cohesionless material and dissipational energy, one will obtain a case which will be similar to a purely kinetic model in which the kinetic energy of the entrained material equals the energy supplied by the jet. In this case, one obtains:

$$\frac{\mathrm{d}}{\mathrm{d}t}(\text{kinetic energy}) = \text{Rate of work supplied by the jet} \tag{51}$$

An application of the results from Eqs. (46)–(49) in Eq. (51) leads to a rather simple analytical equation given by:

$$FC\cos(\varphi_0 + \varphi_1) == \frac{1}{2}\rho^* C^2 SC \tag{52}$$

so that

$$C^2 = \frac{2F}{\rho^* S}\cos(\varphi_0 + \varphi_1) \tag{53}$$

When Eq. (44) is utilized in Eq. (53), we finally obtain

$$C = \sqrt{\frac{4}{27}\frac{\rho}{\rho^*}\left(\frac{gH_c^2}{S}\right)\cos(\varphi_0 + \varphi_1)} \tag{54}$$

This relationship shows that the rate of head cut migration for a given critical horizontal thrust by the flow is inversely related to the square root of the head cut size. Conversely, for a given head cut size migration is quadratically related to the critical flow depth.

For the sake of a qualitative evaluation, if we assume $\rho/\rho^* = 1/2$, $S/H_c = 10$, and cos $(\varphi_0 + \varphi_1) = \cos 75°$, we obtain from Eq. (54)

$$C \approx 0.044 V_c \tag{55}$$

Eq. (55) is derived by making many simplifying assumptions and, therefore, establishes certain scaling law with the magnitude of overland flow velocity. This finding appears to be in confirmation with results of the set of experiments carried out in Bennett et al. (2000). Eq. (48), however, forms a basis for testing the role played by the characteristics of soil dynamical parameters. The surface flow (hydraulic) parameters also are represented in Eq. (54). Eq. (55), however, is a simplification of the dynamics of head cut which, however, retains the kinetic aspects of the system.

6. Summary

This paper describes a conceptual approach of head cut growth based on continuum mechanical principles. These principles consist of the energy balance in the head cut region in which the flow energy is converted into head cut growth. An energy model was formulated that applies to any process region where erosion by surface flow is taking place. Of the different head cut modes that occur in nature, the one with a cohesive surface layer on top of a cohesionless substrate was further investigated. A condition for head cut growth was derived in which the critical flow velocity was related to the surface layer mechanical and physical properties. This relationship appears to have applicability to cases when incipient rilling occurs. For studying the dynamic equilibrium of head cut movement, the energy principle enables us to examine the roles played by the hydrodynamic parameters of surface flow and the soil mechanical parameters. Under simplifying assumptions, it is seen that the steady state head cut growth velocity bears a direct relationship with the critical surface flow velocity.

List of Symbols

A	cross-sectional area of head cut of application case
C	rate of head cut migration
E	internal energy
E_y	Young's modulus of elasticity
F_{cr}	critical hydraulic thrust
H	water depth of flow
H^*_{cr}	critical water depth at tip of seal
H_{cr}	critical water depth
H'	energy terms other than kinetic and internal, associated with erosion processes
I	moment of inertia
K	kinetic energy per unit mass
K_1	kinetic energy per unit width of enclosed volume of application case
M	bending moment
M_u	ultimate (plastic) moment
P	time rate of erosion energy for detached soil
Q	heat energy rate entering the process region
R	rate of flow energy
S	head cut depth per unit width of application case
S_c	eroding surface area
S_ρ	arbitrary surface delineating the process region
T	Total kinetic energy
$\boldsymbol{T}_i$ $(i=1, 2, 3)$	surface traction vector
V_c	critical water velocity
V_p	volume of process region
W	work
X_i (1,2,3)	fixed coordinates
b	seal width
e	internal energy per unit mass
$\dot{e}$	time rate of change of internal energy per unit mass
e_{ij}	strain tensor
$\dot{e}_{ij}$	time rate of change of strain tensor
$\boldsymbol{e}_r$	unit vector
$\boldsymbol{f}_i$ $(i=1, 2, 3)$	body force vector

g gravitational acceleration
h seal thickness
ℓ length of seal overhang
$\boldsymbol{n}_i$ outward normal vector
q total weight per unit length of seal (soil weight plus water load)
$\vec{q}_i$ heat flux vector
q_0 soil weight per unit length
r length of vector $\vec{r}$
$\vec{r}(\theta, t)$ position vector
t_{ij} stress tensor
u strain energy
$\boldsymbol{u}_i$ displacement vectors
$\dot{u}_i$ time rate of change of displacement
u_{ij} velocity gradient
$\ddot{\boldsymbol{u}}_i$ $(i = 1, 2, 3)$ acceleration vector
γ heat produced by internal heat sources
δ deflection from horizontal of seal tip
ω_3 angular velocity
φ jet flow angle with horizontal coordinate
Φ angle of seal deflection at the "plastic" hinge
θ relational angle of (x_1,x_2)-coordinate system into the (X_1,X_2)-coordinate system
ρ fluid mass density
ρ^* mass density of eroding material (soil + water)
σ_y yield stress

Acknowledgements

The authors are deeply indebted to Dr. Calvin Rose of Brisbane, Australia, who read the manuscript and found several errors and made numerous suggestions which significantly improved the manuscript.

References

Bennett, S.J., Alonso, C.V., Prasad, S.N., Römkens, M.J.M., 2000. Experiments on head cut growth and migration in concentrated flows typical of upland areas. Water Resour. Res. 36 (7), 1911–1922.
Budiansky, B., Rice, J.R., 1972. Conservation laws and energy release rates. ASME J. Appl. Mech. 40, 201–203.
Eringen, A.C., 1980. Mechanics of Continua. R.E. Kreiger Publ., Huntington, NY, p. 123.
Freund, L.B., 1972. Energy flux into the tip of an extending crack in an elastic solid. J. Elast. 2 (4), 341–349.
Henderson, F.E., 1965. Open Channel Flow. MacMillan Publ., NY. p. 52, 193.
Moore, W.L., 1943. Energy loss at the base of a free overfall. Trans. ASCE 108, 1343.
Römkens, M.J.M., Prasad, S.N., Gerits, J.J.P., 1997. Soil erosion modes of sealing soils: a phenomenological study. Soil Technol. 11, 31–41.
Timoshenko, S.P., Gere, J.M., 1961. Theory of Elastic Stability. McGraw-Hill, New York, NY.
Witham, G.B., 1973. Linear and Non-Linear Waves. Wiley, New York, NY.